High polarization purity 0.1 – 0.3 THz FSS Polarizer in reflection

Roberto Garrote Moreno[(1)], Alvaro Fernández Tuesta[(2)], Miguel A. Salas-Natera[(1)], Jorge Teniente Vallinas[(3, 4)], Carlos Martínez Herreros[(2)]. Ramón Martínez Rodríguez-Osorio[(1)]
E-mail roberto.garrote@alumnos.upm.es, miguel.salas@upm.es, jorge.teniente@unavarra.es.
[(1)] Centro de Procesamiento de Información y Telecomunicaciones, Escuela Técnica Superior de Ingenieros de Telecomunicación. Universidad Politécnica de Madrid, 28040, Madrid, Spain
[(2)] Universidad Politécnica de Madrid, 28040, Madrid, Spain.
[(3)] Departamento de Ingeniería Eléctrica, Electrónica y de Comunicación. Universidad Pública de Navarra, 31006, Pamplona, Spain.
[(4)] Instituto de Smart Cities, Universidad Pública de Navarra, Pamplona, 31006 España

***Abstract*- The motivation behind the research lies in the necessity to identify indoor applications for 6G to contextualize and render practicality to the proposed work. While terahertz communication holds promise for achieving ultra-large bandwidths and Tbit/s speeds, the primary challenge lies in implementing transceivers suitable for integration into indoor and pico-cells WLANs for 6G applications. The proposed FSS architecture addresses these challenges by introducing a low-profile design that not only overcomes volumetric constraints but also reduces system complexity, thus enhancing cost-effectiveness and facilitating mass adoption across diverse technological domains. This innovative approach enables the implementation of dual polarization in both Co-Polar (CP) and Cross-Polar (XP) operations without the need for intricate multiport networks, thereby simplifying the system architecture and enhancing its versatility. The FSS design offers ultra-large bandwidth circular polarization fields in reflection mode, capable of providing two separate bands for each circular polarization, making both CP and XP operations feasible with minimal changes in phase, thereby paving the way for future 6G communications systems.**

I. INTRODUCTION

The new trend in Antenna design is to move to the THz band, where multiple applications will be developed soon, for example in satellite communications [1], ISL communications are going to use up to 200GHz. Also, it is known that 6G generation is going to operate at THz bands [2, 3], that lies between the mmWave and infrared frequencies, and is considered a solution to achieve Tbit/s thanks to the ultra-large bandwidth.

In terms of FSS technology, one limitation presented in the state of art in order to obtain sub-THz designs is the manufacture technique, being this a major problem, for this reason, another novelty presented in this paper is the use of quartz dielectric material acting as substrate, and an innovative manufacturing technique using photolithography and e-beam deposition of materials, where precision in the order of 1µm can be achieved.

The transition from conventional limitations outlined in the State of the Art (SoA) to the implementation of the proposed Frequency Selective Surface (FSS) architecture bears significant implications at the system level. The SoA constraints, predominantly revolving around complexities in profile, cost, and feed-chain configurations, have been formidable hurdles in achieving optimal performance in high-frequency applications.

The motivation behind this work stems from the need to explore indoor applications for 6G technology to contextualize and provide practical utility to the research. Terahertz communication, while promising for its potential to achieve ultra-large bandwidths and Tbit/s speeds, faces a significant challenge in implementing transceivers suitable for integration into indoor WLANs for 6G applications. Moreover, due to the high frequency of terahertz bands, there are considerable free space losses, making indoor applications, such as medical or video, preferred for their feasibility in this context [4].

In addressing the limitations of the state-of-the-art (SoA) technology, particularly in Frequency Selective Surface (FSS) architectures, significant implications at the system level are anticipated. The proposed FSS architecture offers a paradigm shift by overcoming constraints in profile complexities, costs, and feed-chain configurations. Its low-profile design not only addresses volumetric constraints but also reduces system complexity, translating into cost-effectiveness crucial for widespread adoption across diverse technological domains.

Furthermore, the innovation lies in the feasibility of implementing complex dual polarization in both Co-Polar (CP) and Cross-Polar (XP) operations without the need for intricate multiport networks in the feed-chain. This simplifies the system architecture while enhancing versatility and adaptability in accommodating diverse polarization requirements. By mitigating complexities associated with feed-chain configurations and enabling dual polarization capabilities, the proposed FSS offers a leap forward in functionality without compromising performance, revolutionizing systems reliant on high-frequency electromagnetic manipulation.

Regarding the implementation of the design, manufacturing at sub-THz frequencies requires precision, with deviations of less than 1µm achieved in this work. Validation of the design at sub-THz frequencies, particularly from 0.16 THz to 0.3 THz, necessitates a quasi-optical setup, presenting calibration and measurement challenges. Different polarizer designs in reflection mode have been explored, with the proposed approach consisting of a single slotted patch FSS capable of providing ultra-large bandwidth circular

polarization fields for future 6G communications systems. This design offers two separated bands for the two circular polarizations fully usable for XP operation, with feasible CP operation as well, ensuring versatility and adaptability in meeting the demands of emerging communication technologies.

The proposed FSS architecture introduces a paradigm shift by addressing these limitations. Its low-profile design not only tackles the volumetric constraints faced in previous configurations but also offers a pathway towards achieving reduced system complexity. This reduction in complexity directly translates into cost-effectiveness, a pivotal factor in mass adoption and implementation across various technological domains.

Moreover, the innovation lies in the feasibility of implementing complex dual polarization in both Co-Polar (CP) and Cross-Polar (XP) operations without resorting to intricate multiport networks in the feed-chain., which increase the weight and the complexity of the integration of the full system. This feature is revolutionary, as it not only simplifies the system architecture but also enhances its versatility and adaptability in accommodating diverse polarization requirements.

By mitigating the complexities associated with feed-chain configurations and enabling dual polarization capabilities, the proposed FSS offers a leap forward in functionality without compromising performance.

II. PRINCIPLE OF OPERATION

The proposed FSS circular polarizer in reflection mode offers versatile operation in both Co Polarization (CP) and Cross Polarization (XP) modes, providing two distinct colors for each frequency band. By decomposing the incident field into orthogonal components and shifting one by 90 degrees, the FSS achieves Right-Hand Circular Polarization (RHCP) and Left-Hand Circular Polarization (LHCP) reflections at different frequencies for both TE and TM modes. Additionally, the FSS can generate four colors by decomposing the incident field into TE and TM components, with phase differences and equal amplitudes, facilitating CP and XP operations at multiple frequencies.

Furthermore, the FSS achieves CP operation by decomposing the incident field into orthogonal components, with phase shifts introduced by the patch perimeter. This innovative design enables RHCP and LHCP reflections at different frequencies, with the option for XP modes with the two senses of polarization. This principle allows for the generation of four distinct colors (2xPolarizations and 2xFrequencies), enhancing the versatility and adaptability of the FSS in meeting the requirements of various communication applications.

For CP mode, Fig. 1 the FSS decomposes the incident linearly polarized field in the two orthogonal components, TE and TM, with a phase difference of 90º and equal amplitude. Thus, by using the TE mode the reflected field is RHCP at f1 and f2, while by using the TM mode the reflected field is LHCP at f1 and f2.

For XP mode, in Fig. 2, the FSS decompose the incident linearly polarized field in the two orthogonal components, TE and TM, with a phase difference of 90º and equal amplitude. Thus, by using the TE mode the reflected field is LHCP at f1 and RHCP at f2, while by using the TM mode the reflected field is RHCP at f1 and LHCP at f2.

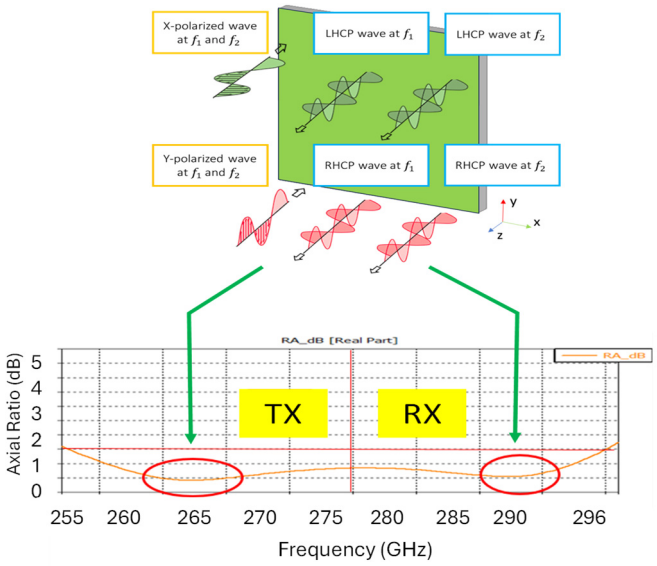

Fig. 1. CP mode operation.

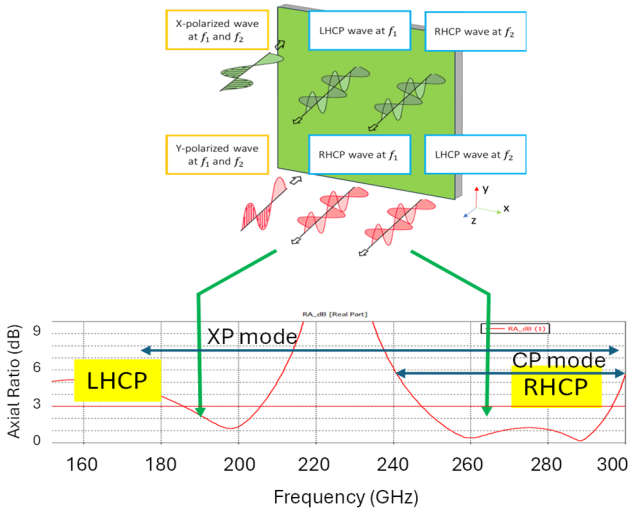

Fig. 2. XP mode operation.

III. FSS POLARIZER DESIGN

The Design of the polarizer FSS, Fig.3 in reflection mode has been presented before [5]. This design consists in just one layer, excited with a linear TE or TM mode, that is decomposed into two orthogonal components and delayed 90º each, so the reflected wave is circularly polarized. One main advantage of this model is that it presents a very low profile, only 0.17 mm dielectric thickness.

A novelty presented in this work is the use of quartz glass [6] as dielectric material of the polarizer. The Fig. 4.a shows the axial ratio between 150-300GHz and the phase difference between the TE mode and TM mode vectors, when the TE vector excites the surface, showing that there are two different areas, where the axial ratio changes its senses of polarization, as we can see in the phase response (Fig. 4.b).

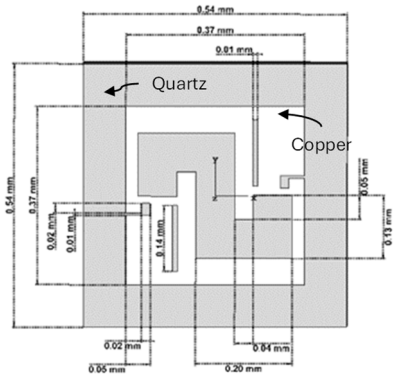

Fig. 3. Unit cell of the proposed design.

As part of the polarizer cell design procedure, the figures below are presented to define the frequency position of the axial ratio minima for operating in Co-polar mode. For this discussion, only the axial ratio for right-handed circular polarization (RHCP) is presented, where we observe the frequency of the minimum axial ratio for an internal or external perimeter in wavelength normalized units with respect to that frequency. Additionally, the axial ratio of the minimum in each case is represented, as shown in CST and the minimum achievable axial ratio with the mentioned data.

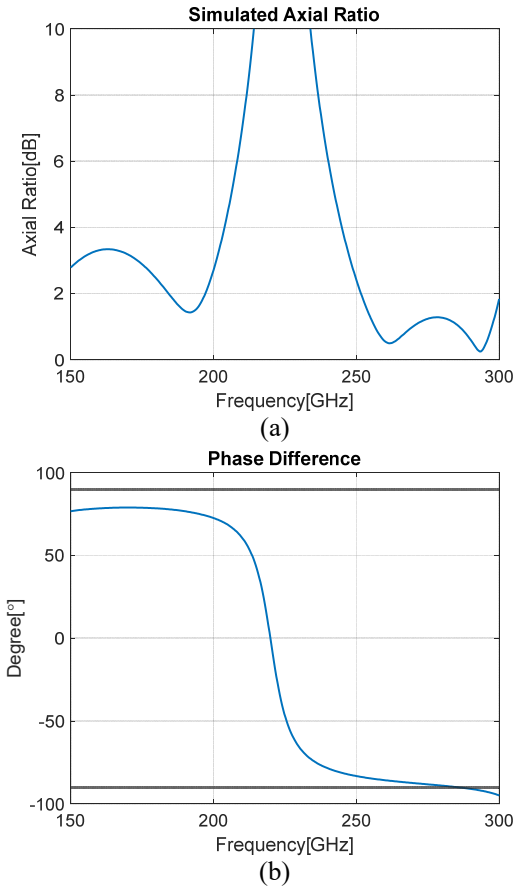

Fig. 4. Simulated axial ratio (a) and phase difference of the TE and TM reflected modes (b).

It is important to emphasize that the cell has elements that provide sufficient degrees of freedom to optimize the axial ratio further at each point, but the curves allow for an initial design with an axial ratio less than or equal to 1 dB. Fig. 5.a illustrates the impact of the outer perimeter, where variations of the perimeter describing the length and width of the metallic patch modify the frequency at which the minimum axial ratio occurs at the bottom of the band, while keeping the rest of the parameters unchanged. Similarly, Fig. 5.b shows the impact of the S-shaped inner perimeter, where variations of the perimeter describing the S-shaped slot of the patch modify the frequency at which the minimum axial ratio occurs at the top of the band, also keeping the rest of the parameters unchanged.

The frequencies for the outer (1) and inner (2) perimeters can be modelled by a quadratic function as follows.

$$f_o = 0.13p_o^2 - 25p_0 + 1.4x10^3 \quad (1)$$

$$f_i = 1.3p_i^2 - 99p_i + 2.1x10^3 \quad (2)$$

Where f_o is the frequency for minimum axial ratio for outer perimeter, f_i is the frequency for minimum axial ratio for inner perimeter, p_o is the outer perimeter, and p_i is the inner perimeter.

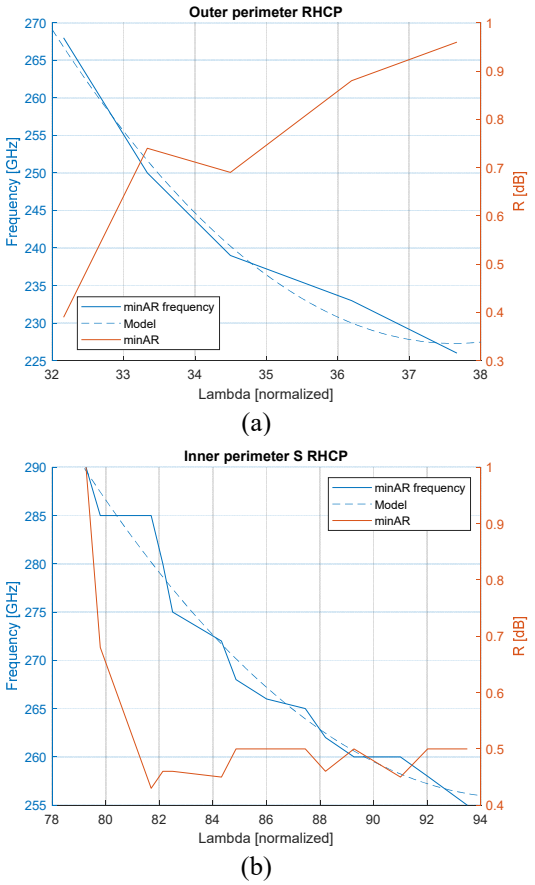

Fig. 5. Frequencies for minimum axial ratio as a function of the outer perimeter of patch (a) and of the inner perimeter of the S slot (b)

IV. Manufacture and Measurement

The proposed design was manufactured and measured by the Public University of Navarra, using photolithography and e-beam deposition for the manufacture process and a quasi-optical test setup for the measurement campaign, see Figs. 6 and 7. The photolithography technique uses a maskless aligner for circuit patterning and allows the realization of models with 1 µm of precision, as this model at the upper part of the mm-wave band requires.

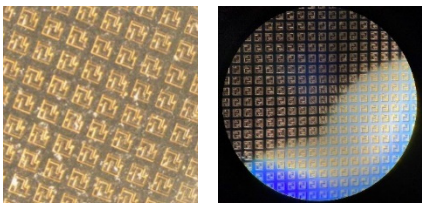

Fig. 6. Manufactured model (microscope view)

The fabricated model has been independently measured in two frequency bands. First from 175 GHz to 200 GHz, Fig. 8, using WR5.1 mmwave frequency extenders where the model behaves similarly to the simulation, but with a worsening of the axial ratio, reaching its minimum value at 188GHz, with a value of 2.8dB.

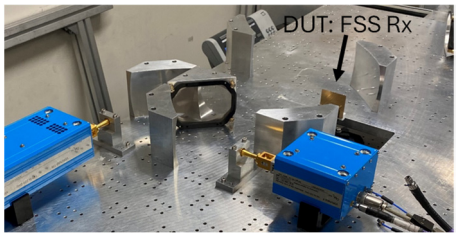

Fig. 7. Measurement setup

Then, the measurements were done for the frequency range from 200 GHz to 300 GHz using WR3.4 mmwave frequency extenders. In this sense valid frequency ranges are [175 – 210 GHz] and [245 – 270 GHz], but measurements were realized for a more extended range as observed in the results of Fig. 8 and Fig. 9, respectively. Fig. 8 shows that the FSS provides axial ratio better equal than 5 dB in the frequency range of [177.5 – 192.5 GHz].

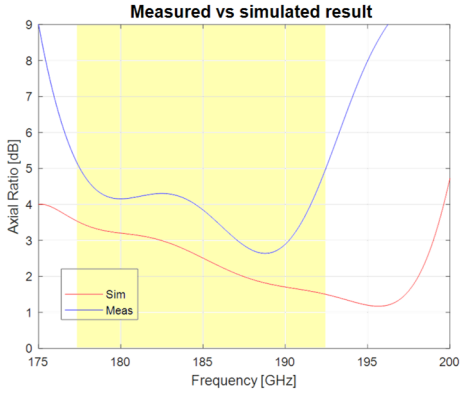

Fig. 8. Simulation and measured (175-200GHz)

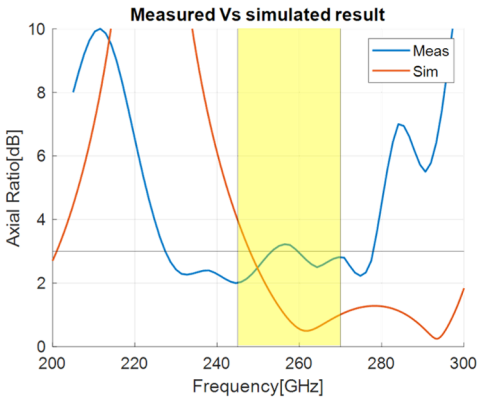

Fig. 9. Simulation and measured (200-300GHz)

Besides, note that for the second range, where the model presents a higher bandwidth and an optimized response in terms of axial ratio, the measurements have a higher similarity with respect to the simulated. The last resulting in a performance with axial ratio values better than 3dB between 221-270GHz approximately.

These are good results that demonstrate the technological feasibility since the simulation and the measurement match with a difference less equal to 1 dB of axial ratio into the significant frequency range highlighted in yellow. This is much more important when considering the difficulties that the manufacture and measurement of this type of devices presents in such a high frequency band.

V. Conclusions

In this work we have explored the design of a polarizing FSS in reflection mode in the 0.1-0.3THz band, using innovative materials such as quartz as substrates of the structure. Likewise, the model has been manufactured by photolithography and e-beam deposition of material and has been measured in the bands from 175GHz to 300GHz, having positive results in measurements. The deviation observed in the significant frequency band in term of axial ration is less than ~1 dB obtaining overall axial ratio lower than 3 dB for CP mode and lower than 4 dB for XP mode of operation. The frequency shift due to manufacturing imperfections is negligible thanks to the great bandwidth of the FSS design and to the accuracy achieved in the manufacturing process.

Acknowledgements

This work was supported by the Spanish Government, Ministry of Economy, National Program of Research, Development and Innovation under the project New Array Antenna Technologies and Digital Processing for the FUTURE Integrated Terrestrial and Space-based Millimeter Wave Radio Systems - UPM-InTerSpaCE (PID2020-112545RB-C51).

References

[1] M. Civas y O. B. Akan, «Terahertz Wireless Comuniations in Space,» *ITU Journal on Future and Evolving Technologies,* 2021.

[2] H. Chen, H. Sarieddeen, T. Ballal, H. Wymeersch, M.-S. Alouini y T. Y. Al-Naffouri, «A Tutorial on Terahertz-Band Localization for 6G Communication Systems,» *IEEE Communiation Surveys & Tutorials,* vol. 24, nº 3, 2022.

[3] A. Shafie, N. Yang, C. Han, J. M. Jornet, M. Juntti y T. Kurner, «Terahertz Communications for 6G and Beyond Wireless Networks: Challenges, Key Advancements, and Opportunities,» *IEEE Network,* vol. 37, nº 3, 2023.

[4] S. Tripathi, N. V. Sabu, A. K. Gupta y H. S. Dhillon, «Millimeter-wave and Terahertz Spectrumfor 6G Wireless,» de *6G Mobile Wireless Networks*, 2021, pp. 83-121.

[5] R. G. Moreno, M. A. Salas-Natera y R. Martínez, «Low profile dual-band linear-to-circular polarization FSS for satellite,» *XXXVII Simposio Nacional de la Unión Científica Internacional de Radio,* 2022.

[6] P. A. Sarafis y A. G. Nassiopoulou, «Dielectric properties of porous silicon for use as a substrate for the on-chip integration of millimeter-wave devices in the frequency range 140 to 210 GHz,» *Nanoscale Research Letters,* 2014.